Interaction of the Antitumor Drug 9-Aminoacridine with Guanidinobenzoatase Studied by Spectroscopic Methods: A Possible Tumor Marker Probe Based on the Fluorescence Exciplex Emission†

Adrian Murza,‡ Santiago Sánchez-Cortés,*,§ José V. García-Ramos,§ José M. Guisan,‡ Carlos Alfonso,|| and Germán Rivas||

Instituto de Catálisis, CSIC, Campus UAM-Cantoblanco, 28049 Madrid, Spain, Instituto de Estructura de la Materia, CSIC, Serrano, 121, 28006 Madrid, Spain, and Centro de Investigaciones Biológicas, CSIC, Velázquez, 144, 28006 Madrid, Spain

Received March 14, 2000; Revised Manuscript Received May 30, 2000

ABSTRACT: Fluorescence spectroscopy, surface-enhanced Raman spectroscopy (SERS), and analytical centrifugation are applied in this work to study the interaction of the antitumor drug 9-aminoacridine (9AA) with a trypsin-like protease, guanidinobenzoatase (GB), extracted from an Erlich tumor. As a consequence of this interaction, a strong 9AA exciplex emission can be detected at a certain drug and enzyme concentration. The 9AA exciplex emission was also studied for 9AA interacting with others serin proteases: α-chymotrypsin, trypsin, and penicillin G-acylase (PGA), as well as with bovine serum albumin (BSA) in order to obtain information about the active center of GB. We have found that the exciplex 9AA emission may be induced by a ring-stacking interaction between the monomeric drug, under the amino form, and an aromatic residue placed in the catalytic site of the protein. The results derived from Raman spectroscopy corroborate this interaction mechanism, as demonstrated by the existence of typical protonated amino 9AA marker bands as well as an important modification of the ring vibrations, thus indicating the existence of an interaction through ring stacking. The analytical centrifugation technique was applied to study the GB association in aqueous solution, demonstrating that the 9AA/GB interaction depends on the enzyme quaternary structure. An interaction of 9AA with an associate form of GB, which may be the actual enzyme active form, is suggested.

Guanidinobenzoatases (GB)[1] represent a trypsin-like protease family related with tumor processes. These enzymes are located on the membrane surface of the tumor cells and play a crucial role in cell mobility and metastasis. Previous studies have shown that GB proteolytic activity against fibronectin (*1*), collagen (*2*), and zymogen (*3*) gives rise to a rapid degradation of the connective tissue, favoring the tumor cell displacements. At the cell membrane, GB is in a latent state inactivated by its interaction with a protein inhibitor produced by the own cell (*4*).

9-Aminoacridine (9AA) (Figure 1) is an antibacterial, mutagenic (*5, 6*), and antitumor drug (*7, 8*) that has been proposed as a specific fluorescent probe capable of binding the active center of GB. In fact, the staining of 9AA in histopathological sections has been used to locate malignant cells in many tumor tissues (9−*15*). Steven et al. (*1*) observed a notable shift of the cell fluorescence from blue−green to yellow−orange, that may indicate the formation of 9AA excimers in these cells. 9AA can dimerize in aqueous solution at high drug concentrations, giving rise to an excimer emission at about 535 nm (*16*). Owing to this, the study of the interaction mechanism of 9AA with GB could be of a great interest due to the possibility of using this fluorescent marker for detecting and inhibiting tumors, as well as obtaining more active inhibitors of this enzyme involved in tumor processes. In this respect, the influence of cellular specific inhibitors of GB in the 9AA/GB interaction is also interesting, regarding the metastasis process and the start of cell mobility, and should also be investigated in order to check the ability of 9AA to bind to GB in vivo and the possibility of detecting the metastasis in the earlier tumor expansion stages.

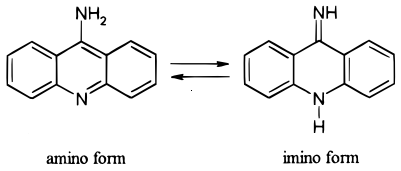

FIGURE 1: Tautomer equilibrium in 9-aminoacridine (9AA).

† This work was supported by Grant PB97-1221 (Dirección General de Enseñanza Superior e Investigación Científica). We acknowledge The Consejo Superior de Investigaciones Científicas for a contract to S.S.-C. We also acknowledge MEC (Ministerio de Educación y Cultura) and Schering-Plough S.A for a fellowship to A.M.

* Corresponding author. Fax: + 34 91 564 55 57. Tel: + 34 91 561 68 00. E-mail: imts158@iem.cfmac.csic.es.

‡ Instituto de Catálisis.

§ Instituto de Estructura de la Materia.

|| Centro de Investigaciones Biológicas.

[1] Abbreviations: SERS, surface-enhanced Raman spectroscopy; SERRS, surface-enhanced resonance Raman spectroscopy; IR, infrared; 9AA, 9-aminoacridine; GB, guanidinobenzoatase; PGA, penicillin G-acylase; BSA, bovine serum albumin; SDS−PAGE, sodium dodecyl sulfate−polyacrylamide gel electrophoresis; NPGB, *p*-nitrophenyl-*p*-guanidinobenzoate.

10.1021/bi000583p CCC: $19.00
Published on Web 08/04/2000

Vibrational spectroscopies (IR, Raman) provide specific molecular information that is very useful in recognizing processes such as the 9AA/GB interaction. A vibrational spectrum is composed of bands associated with characteristic vibrations of particular groups of atoms, which are defined by specific ranges of frequency and intensity in the IR and Raman spectra. However, studies in aqueous media seriously limit the use of IR spectroscopy, while the presence of strongly fluorescent compounds, such as 9AA, limits the application of Raman spectroscopy. Nevertheless, a recent technique related to Raman spectroscopy, surface-enhanced Raman spectroscopy (SERS), can be used to carry out Raman studies of very fluorescent molecules in aqueous media and at low concentration (*17*). For this reason, we have employed the SERS technique as well as steady-state fluorescence spectroscopy to elucidate the mechanism of the 9AA/GB interaction.

In a previous work (*16*), we have applied the fluorescence and SERS spectroscopy to study the aggregation and excimer emission of 9AA in aqueous solution. Fluorescence data indicated that the excimer emission is connected to the dimerization of this drug in solution: the formation of 9AA dimers is greatly favored when the drug is under the amino form at neutral and acidic pH, while at alkaline pH the imino 9AA form tends to form large-sized aggregates which cannot be excited to render excimer emission. Moreover, an attribution of the main Raman features appearing in the Raman spectra was proposed, providing marker Raman bands of the amino and imino 9AA tautomers. The results found in this previous work have been very useful for interpreting the 9AA/GB Raman spectra.

Since the structure of the active site of GB has not been yet reported, the interaction of 9AA with other serine-active enzymes such as penicillin G-acylase (PGA), trypsin, and α-chymotrypsin, which display a similar catalytic activity, has been also investigated to afford more information about the GB active site structure and the 9AA−GB photodynamic mechanism. Moreover, the interaction with bovine serum albumin (BSA) was also checked as this carrier protein interferes in the purification of GB from the biological fluids employed as GB sources (*18*).

The quaternary structure of GB is an important factor which determines its biological activity as well as its capability of interaction with ligands. Electrophoresis experiments (*14*) showed that GB of renal carcinoma spontaneously tetramerize in solution. This multimer association induces a structural change as well as a variation of the catalytic activity of GB. Consequently, the different structures of the active center may exist in the associated state, and monomeric GB may manifest different affinities toward 9AA. In recent works, it has been proved that the interactions between the individual enzyme subunits imply hydrophobic and/or ionic bonds. For this reason, the sodium dodecyl sulfate−polyacrylamide gel electrophoresis (SDS−PAGE) technique, employed so far to characterize and purify this enzyme, may induce enzyme denaturalization with loss of quaternary structure. There are many examples of enzymes for which dissociation into dissimilar subunits has been demonstrated merely by dilution (*19, 20*). In this sense, the analytical ultracentrifugation has been used in this work to analyze GB polymer association as a function of the protein concentration and the influence of the drug in the association process.

MATERIALS AND METHODS

Materials. Six percent cross-linked agarose beads were from Hispanagar Co. (Burgos, Spain). Two different GB sources were used for 9AA/GB interaction studies: ascitic fluid of mouse Ehrlich tumor, provided by Dr. J. L. Subiza from San-Carlos Universitary Hospital in Madrid; and human melanoma line A375 cells, extracted from metastatic melanoma, obtained from the Department of Immunological Oncology, Hospital General Universitario Gregorio Marañon (Madrid). 9-Aminoacridine hydrochloride (9AA) and *p*-nitrophenyl-*p*-guanidinobenzoate (NPGB) were purchased from Sigma Chemical Co. (St. Louis, MO). All the reagents were analytical grade.

GB Purification. GB for in vitro studies was extracted from the ascitic fluid of a mouse Ehrlich tumor, and purified by using an agmatine-CH Sepharose 4B affinity column as described in reference (*18*). In the last work, a double purification strategy based on the use of mimetic matrixes as well as soluble mimetic ligands is described. The specific enzymatic activity, and the end of the purification process, was 0.92 unit/mg [total activity (units/mL)/protein concentration (mg/mL)], that represented a purification factor of 250 with respect to the initial crude preparation. The activity of GB was assayed by using NPGB as substrate, measuring the increment of absorbance at 348 nm. One activity unit represents the amount of GB able to hydrolyze 1 μmol of NPGB.

Briefly, the purification of GB consisted of a preliminary purification step where a large amount of the contaminant proteins (mainly albumin) present in the crude extract was removed by using mimetic matrixes (which trap and adsorb albumin but not GB). In a second affinity purification step, the resulting unbound proteins (prepurified GB) were offered to the affinity matrix, in the presence of a mimetic soluble ligand. The mimetic ligand avoids the binding of competing contaminant proteins, but allows the binding of GB on the affinity matrix. The enzyme elution from the affinity column was carried out in the presence of soluble substrate, NPGB. Soluble GB containing hydrolyzed substrate was subjected to gel filtration through a Sephadex G-25 (PD-10) column in order to obtain a separate GB solution from the substrate. Purified GB was lyophilized and freeze-dried.

Human Melanoma Cell Culture and Staining with 9AA. Human melanoma cells were grown as monolayers as described elsewere (*21, 22*). Briefly, cells were seeded in 75 cm^3 culture tubes and maintained under a humidified atmosphere with 5% CO_2 at 37 °C. The RPMI 1640 medium supplemented with 3 mL of glutamine, 100 mL of 10% fetal calf serum, and 10 mL of streptomycin/penicillin per liter was employed. When a density of 10^6 cells/cm^2 was attempted, cells were recultured on culture slides, dried, and stained for the fluorescence experiments.

A cellular DNA prestaining step with hematoxylin (*23*) was necessary to eliminate possible interferences in the fluorescence experiments, owing to the demonstrated affinity of 9AA for the base pairs of the DNA (*5*). The 9AA staining of melanocytes containing the cytoplasmic GB inhibitor and the elimination of the GB inhibitor were carried out by the methods described by Steven et al. (*1*).

Human Melanoma GB Inhibitor Purification. Washed cultured malignant melanoma cells (tumoral cell line A 375)

were used as a source of the cytoplasmic inhibitor of GB, by using a method described by Steven et al. (*4*). The GB−inhibitor complex was displaced from the cell surface by fibrin fibrils formed from fibrinogen and added thrombin. The fibrin fibrils bound GB, while the inhibitor remains in the solution fraction. After removing the fibrils with GB, we obtained a solution containing the inhibitor.

Fluorescence Spectroscopy. Samples for 9AA fluorescence measurements were obtained from an initial 10^{-2} M 9AA aqueous solution prepared in 10 mM phosphate buffer at pH 7 by dilution to the desired final concentration.

Samples for fluorescence measurements on the 9AA/GB complex were prepared by mixing 9AA and lyophilized GB in 10 mM phosphate buffer at pH 7, from an initial 30 mM GB solution in phosphate buffer at pH 7, up to the desired concentration. Solution compounds were allowed to react for 10 min before each fluorescence measurement. The same experimental procedure was carried out with the others proteins tested here: α-chymotrypsin, trypsin, PGA, and BSA. Excitation and emission spectra were recorded with a Perkin-Elmer LS 50 B spectrometer. Quartz cuvettes of 1 cm were used.

For fluorescence experiments carried out on melanoma culture cells, dried cultured melanocytes deposited on a glass slide were employed with an attached mirror to the opposite side of the slide. Then, these slides were placed at a 60° angle orientation with respect to the excitation light.

Surface-Enhanced Raman Spectroscopy. SERS measurements were carried out on silver colloids prepared using the Lee−Meisel method (*24*), in the following way: 200 mL of a 10^{-3} M $AgNO_3$ aqueous solution was heated to boiling, 4 mL of a 1% trisodium citrate solution was then added, and the mixture was kept boiling for 1 h.

For SERS measurements of the complex, GB aqueous solutions in the range 10^{-6}−10^{-5} M were prepared from the lyophilized enzyme, in 30 mM phosphate buffer, at pH 7. The 9AA solution was prepared by dissolving 9AA-hydrochloride in water up to a 10^{-2} M concentration. The 9AA−GB complex was prepared by mixing adequate volumes of the above 9AA and GB aqueous solutions, up to a 1/10 (9AA/GB) molecular ratio. The control sample (9AA without GB) was prepared in the same way by mixing the 9AA aqueous solution with a water volume equal to that of the GB solution employed for preparing the complex. An aggregated Ag colloid was then added to these solutions (blank and complex), in such a way that the final 9AA concentration was 10^{-6} or 10^{-7} M both in the blank in and the complex, while the GB concentration was 10^{-5} or 10^{-6} M in the complex. The complex was prepared in such a way that the enzyme concentration was 10-fold higher than the drug to ensure a complete interaction of 9AA. The activation of the silver colloid was required for a strong SERS spectrum to be observed. To accomplish that, we have employed KNO_3: 20 μL of a 0.5 M aqueous solution of the salt up to a 10^{-3} M final concentration. After the addition of KNO_3, the suspension become darker and showed a higher optical absorbance at higher wavelengths. The amount of nitrate added in each sample was the same to avoid possible influence of the salt on the spectral profile. The final pH of the mixture was 6.5. The presence in all the samples of Cl^- at the same concentration as 9AA is noted, since the employed drug was 9-aminoacridine hydrochloride.

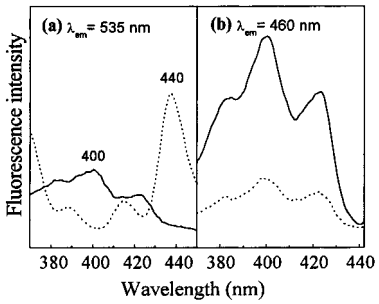

FIGURE 2: Fluorescence excitation spectra of 9AA (10^{-4} M in 10 mM phosphate buffer, pH 7), recorded by fixing the emission at 535 nm (a) and 460 nm (b), at different GB concentrations: 10^{-5} M (dotted line) and 10^{-6} M (solid line).

Normal Raman spectra were recorded in a U-1000 Jovin-Yvon Spectrophotometer by exciting with the 457.9 and 514.5 nm excitation lines provided by a Spectra Physics model 165 argon ion laser. Resolution was set to 4 cm^{-1}, and a 90° geometry was used to record the data. The laser power at the sample was fixed between 20 and 40 mW. Experiments were done by taking one scan with 1 cm^{-1} step size and an integration time of 1 s. FT-Raman spectra were obtained by using a RFS 100/S Brucker spectrophotometer. The 1064 nm line, provided by an Nd:Yag laser, was used as the excitation line. The resolution was set at 4 cm^{-1}, and a 180° geometry was employed with an output laser power of 150 mW. Each FT-Raman spectrum was the result of 1000 scan accumulations recorded for 20 min.

All samples for measurements in either normal Raman or FT-Raman spectrophotometers were placed in 1 mm diameter glass capillaries.

Analytical Ultracentrifugation. Ultracentrifugation measurements were performed in a Beckman Optima XL-A analytical ultracentrifuge equipped with absorbance optics, using an An60Ti rotor. GB was equilibrated in 30 mM phosphate buffer (pH 7). Short column experiments (60−80 μL of protein sample at concentrations ranging from 10^{-6} to 10^{-5} M) were done at two consecutive speeds (6 and 10 krpm) by taking absorbance scans (0.001 cm step size, 4−10 averages) at the appropriate wavelength (280 nm) once the sedimentation equilibrium was reached. Samples were judged to reach the equilibrium by the absence of significant systematic deviations in overlaid successive scans taken for 2 h. We used standard (12 mm optical path) double-sector or six-channel centerpieces of charcoal-filled Epon. The equilibrium temperature was 20 °C. High-speed sedimentation (40 krpm) was conducted afterward for baseline corrections in all the cases. The buoyant molecular mass of the protein was estimated by fitting a sedimentation equilibrium model for a single sedimenting solute to individual data sets with the EQASSOC program supplied by Beckman (*25*). The monomer relative molecular mass was taken as 70 000 Da, deduced from SDS−PAGE experiments, and a value of 41 667 M^{-1} cm^{-1} was used for the extinction coefficient of GB at 280 nm.

RESULTS AND DISCUSSION

Fluorescence Spectroscopy of the 9AA/GB Complex. The steady-state fluorescence excitation spectra of 9AA and the 9AA/GB complex at different enzyme concentrations (10^{-6} and 10^{-5} M) and at pH 7 are shown in Figure 2, and at a

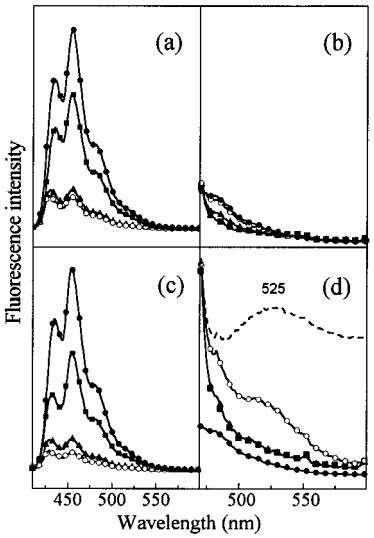

FIGURE 3: Fluorescence emission spectra of 9AA (10 mM phosphate buffer, pH 7) by exciting at 400 nm (a and c) and 460 nm (b and d), at two different GB concentrations: 10^{-6} M (a and b) and 10^{-5} M (c and d), and at variable 9AA concentrations in the 9AA/GB complex: 10^{-6} M (squares); 10^{-5} M (triangles); and 10^{-4} M (open circles). The fluorescence spectra of free 9AA (10^{-4} M) correspond to those marked with solid circles. The dashed line represents the fluorescence difference spectrum between the 9AA/GB complex (10^{-4} M 9AA and 10^{-5} M GB) and 9AA (10^{-4} M).

fixed drug concentration (10^{-4} M). This enzyme concentration dependence was studied by fixing the emission wavelengths at 535 (Figure 2a) and 460 nm (Figure 2b). At a 10^{-6} M enzyme concentration (Figure 2a, solid line), the excitation maximum is observed at about 400 nm. This maximum decreases as the enzyme concentration is increased to 10^{-5} M (Figure 2a, dotted line), thus indicating that the amount of 9AA interacting with GB grows with enzyme concentration. Another effect observed at high enzyme concentration is the excitation maximum red-shift to 440 nm. The band at 400 nm corresponds to the excitation maximum of the monomeric 9AA, while that observed at 440 nm can be related to the formation of the 9AA/GB complex. Moreover, this excitation band is very close to the excitation maximum of the 9AA dimer excimer in aqueous solution, which is observed at 460 nm (*16*, *26*).

Figure 3 shows the emission spectra of the 9AA/GB complex when exciting at 400 nm (Figure 3a) and 460 nm (Figure 3b) at 10^{-6} M GB and different 9AA concentrations, at pH 7. The last excitation lines were chosen because they correspond to the excitation maximum of the 9AA monomer and excimer, respectively. A progressive quenching of the fluorescence intensity is observed in going from higher to lower 9AA concentration (Figure 3a). The spectral profile is dominated preferentially by the bands at 430 and 460 nm, which have been attributed to the 9AA monomer. The magnitude of the fluorescence quenching observed in Figure 3a on increasing the drug concentration does not differ significantly from that observed in the absence of enzyme (spectra not shown). The same behavior was found when exciting at 460 nm (Figure 3b). The absence of an excimer band above 500 nm suggests that at this enzyme concentration, the interaction with 9AA is negligible.

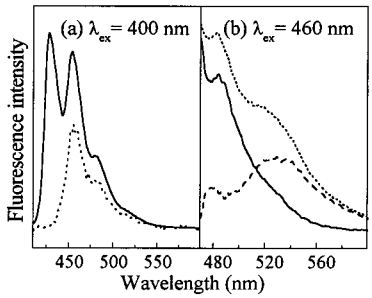

FIGURE 4: Fluorescence emission spectra of malignant human melanoma cell line A375 stained with 9AA before (solid line) and after (dotted line) membrane GB inhibitor elimination. The excitation wavelength was (a) 400 nm and (b) 460 nm. The dashed line represents the difference spectrum between free membrane GB (without inhibitor) and the GB−inhibitor complex in the presence of 9AA.

On the contrary, a notable change in the fluorescence profile occurs when increasing the GB concentration up to 10^{-5} M (Figure 3d). The excitation of the 9AA/GB complex at 460 nm lead to a remarkable increase of the fluorescence above 500 nm with a broad band centered at 525 nm, at a 9AA concentration of 10^{-4} M (open circles), that is better seen in the upper difference spectrum of Figure 3d. The band at 525 nm has been attributed to the excimer emission corresponding to electronic transitions from the excited dimers, in excimers, and heterodimers, in exciplexes, to the corresponding monomers (*27*). The 525 nm emission supports the existence of an interaction of 9AA with GB, which is also corroborated by the marked fluorescence decrease observed for 9AA at the above enzyme concentration when exciting at 400 nm (Figure 3c) as compared to the fluorescence spectra obtained at a lower GB concentration (Figure 3a). To explain the emission at 525 nm in the presence of GB, we suggest that a stacking interaction between 9AA and some aromatic amino acid placed in the active center of GB occurs. This mechanism is more probable than a possible dimerization previous to this interaction with the enzyme. In fact, the differences found by both the fluorescence and SERS spectra between the 9AA dimer and the 9AA/GB complex are arguments against this previous drug dimerization. For this reason, we have considered the emission at 525 nm as an exciplex one, since it is derived from the complex of a monomeric 9AA with GB.

The interaction of 9AA with GB was also analyzed in melanoma line A375 cells. To accomplish such an investigation, it is important to consider that GB is under a latent state due to its interaction with the cell inhibitor (*4*). Figure 4 shows the fluorescence emission spectra of human melanoma cells stained with 9AA, both in the presence and after eliminating the enzyme cytoplasmic inhibitor, at different excitation wavelengths: 400 nm (Figure 4a) and 460 nm (Figure 4b). The emission spectrum obtained at 400 nm shows the bands characteristic of free 9AA at 430 and 460 nm (Figure 4a). The presence of free monomer 9AA in melanoma cells indicates that the drug is not interacting with GB due to its inhibition by the cell inhibitor (Figure 5). A remarkable profile change is observed after removing the cell inhibitor (Figure 4, dotted lines): when exciting at 400 nm, the band at 430 nm completely disappears, while the fluorescence intensity decreases in comparison to the spectrum obtained in the presence of the GB inhibitor (Figure

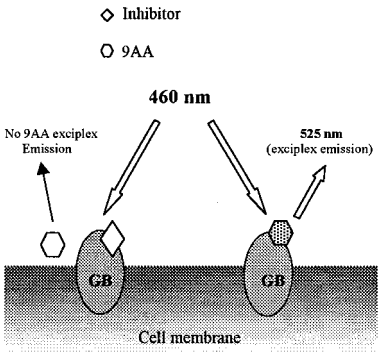

FIGURE 5: Scheme of the different exciplex excitation of 9AA in the presence or absence of GB cell inhibitor.

4a). The excitation at 460 nm gives rise to a broad emission band centered at 525 nm (Figure 4b) assigned to 9AA/GB exciplex emission. This band is better seen in the difference spectrum shown in Figure 4b (dashed line), indicating that on the cell membrane, where GB is localized (9−*13*), the interaction of 9AA with GB favors the exciplex emission. Steven et al. demonstrated that both the cytoplasmic inhibitor and 9AA reversibly interact with the active center of GB (*23*). Thus, the above result indicates that GB interacts selectively with 9AA only after removing the inhibitor (Figure 5). This experiment reveals the specificity of the 9AA/GB interaction in in vivo conditions, even in the presence of other biomolecules, which is of a great importance in relation to the possible use of 9AA as a tumor marker. Furthermore, if the melanoma cells are again treated with the GB cytoplasmic inhibitor, no exciplex emission can be detected, thus demonstrating the reversibility of the 9AA/GB interaction.

Fluorescence Spectroscopy of the Complex of 9AA with Albumin, PGA, Trypsin, and α*-Chymotrypsin.* The interaction of 9AA with BSA and the serin proteases α-chymotrypsin, trypsin, and PGA was also tested by fluorescence spectroscopy (Figure 6). In Figure 6a, the exciplex intensity emission at 525 nm was plotted against 9AA concentration by fixing the protein concentration at 10^{-5} M. For BSA, the fluorescence intensity above 500 nm did not change significantly with the 9AA concentration, thus indicating that the possible interaction with albumin does not give rise to any 9AA exciplex emission. However, for the other proteins, the exciplex 9AA fluorescence emission increases in going from lower to higher 9AA concentration. The exciplex emission increase induced in the presence of these enzymes is more prominent than that observed for the free drug. This suggests that 9AA interacts with the above serine enzymes favoring the 9AA exciplex emission. In the case of BSA, the exciplex emission was even weaker than that observed for the free drug (Figure 6a, diamonds). In Figure 6b, we display the variation of 9AA fluorescence emission recorded at 525 nm against the enzyme concentration at a fixed 9AA concentration (10^{-4} M). This emission increases in going from lower to higher enzyme concentrations, with the exception of BSA, where the emission at 525 nm decreases when the protein concentration is increased (Figure 6b, diamonds). The different behavior observed for BSA in relation to the serine proteases points out the existence of an interaction between 9AA and this protein, although this interaction does not involve the same mechanism as the other proteins tested here.

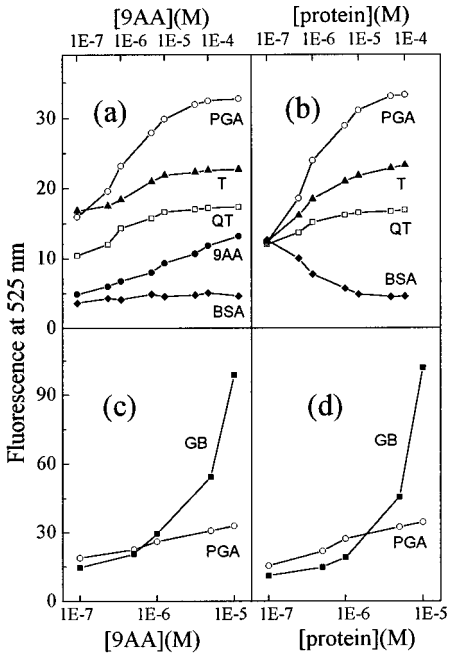

FIGURE 6: (a) 9AA concentration dependence of the fluorescence intensity emission at 525 nm of free 9AA (closed circles) and 9AA in the presence of BSA (diamonds), α-chymotrypsin (CT, open squares), trypsin (T, triangles), and PGA (open circles) in aqueous solution (10 mM phosphate buffer, pH 7) at a fixed protein concentration (10^{-5} M). (b) Protein concentration dependence of the 9AA fluorescence intensity emission at 525 nm in aqueous solution (10 mM phosphate buffer, pH 7) by using a fixed 9AA concentration of 10^{-4} M. (c) Comparison between the 9AA concentration dependence of the fluorescence intensity emission at 525 nm for PGA (open circles) and GB (squares) at a fixed protein concentration (10^{-5} M). (d) Protein concentration dependence of the 9AA fluorescence intensity emission at 525 nm at a fixed 9AA concentration of 10^{-4} M for PGA (open circles) and GB (squares). In all cases, the excitation wavelength was 460 nm.

9AA may interact with BSA under a monomeric form, producing a decrease of emission characteristic of the monomer (data not shown).

The exciplex emission of 9AA when interacting with GB is much more intense than that observed for the other serine proteases. A comparison between the 9AA exciplex emission in 9AA/GB and 9AA/PGA complexes is made in Figure 6c and 6d at different drug and enzyme concentrations. In particular, this emission was about 3-fold more intense at 10^{-5} M GB than that observed for PGA at the same enzyme concentration. Higher GB concentrations could not be investigated due to the small amount of GB available after the purification. This result reveals the enormous ability of GB in inducing the drug exciplex emission and confirms the high selectivity of 9AA in relation to GB.

The exciplex emission observed in the case of the serine enzymes is a consequence of the interaction of 9AA with the active center of these enzymes. The differences observed in the 9AA exciplex emission activity of these enzymes are connected with the different structural characteristics existing in their active centers. Thus, the analysis of the 9AA exciplex emission activity of all these proteins may afford valuable information about the properties of their active centers, in particular that of GB. Several examples of similar studies were also accomplished with other fluorescence probes by other authors (*28*, *29*).

The active site of α-chymotrypsin was found to be very apolar (*30*). Moreover, the only amino acid residues capable of interacting with 9AA through a hydrophobic stacking bond and which could be placed in the vicinity of this enzyme catalytic site are a histidine residue (His 67) and a tryptophan (Trp 215), but they are situated out of the hydrophobic pocket of the active center (*30*). Thus, the interaction of 9AA with this enzyme may mainly involve hydrophobic interaction with aliphatic residues existing in the active center. At these conditions, no significant exciplex emission is expected from the interaction of 9AA with α-chymotrypsin. On the contrary, the active site of trypsin has a less hydrophobic and a more polar character, provided by the presence of an aspartate residue (*31*), which can interact through an ionic bond with positively charged molecules such as the protonated 9AA at neutral pH. 9AA, under the protonated amino form, may interact with this negative center, giving rise to a slight exciplex emission.

The most intense exciplex emission was observed for PGA. It is well-known that the active center of PGA contains an important hydrophobic domain where aromatic residues are located together with a negatively charged aspartate (*32*). This configuration allows a double interaction of 9AA with PGA: (i) ionic interaction via the protonated 9AA with the negative aspartate residue of the active center, and (ii) stacking interaction with the aromatic rings of this active site.

The higher capability of GB to induce exciplex emission when interacting with 9AA, in relation to the other serine proteases, indicates the existence of a negatively charged amino acid, as well as an aromatic residue in the active site of GB, both leading to a strong interaction with 9AA under the amino form. Furthermore, the existence of a negative charge in the active center of GB is also corroborated by the ability of GB to hydrolyze peptidic bonds where a protonated arginine residue is involved (*1*).

Surface-Enhanced Raman Spectra. The SERS spectra of 9AA and the 9AA/GB complex were recorded at several excitation wavelengths: 1064, 514.5, and 457.9 nm. By using the latter excitation wavelength, the SERS spectra can be considered as surface-enhanced resonance Raman spectra (SERRS), as this molecule exhibits an absorption maximum at about 460 nm (*16*), with the advantages that this implies: more sensitivity and selectivity. The use of such an excitation wavelength is advantageous for our purposes, since it enables us the selective detection and study of those 9AA molecules which are interacting with the enzyme. When a SERS experiment involving recognition between a drug and a biomolecule is carried out, one should take into account that the drug acting as ligand could exist under different states: (1) free in the bulk solution; (2) attached to the metal by chemisorption; or (3) close to the metal but not directly linked to it, i.e., physisorbed on the surface or linked to another molecule (interacting with a biomolecule or forming multilayers on the surface). The contribution to the SERS spectrum from molecules of the (1) group is ruled out, since in the presence of the metal surface it is possible to selectively study those molecules which are placed in the vicinity of the metal surface, avoiding the possible contribution of the free 9AA molecules existing in the bulk. In the case of 9AA molecules belonging to the (2) group, their contribution to the SERS spectrum is greatly minimized by selecting a suitable excitation wavelength, through a resonant mechanism. In fact, in a SERS study carried out previously for this molecule (*16*), we have found that a fraction of the adsorbed 9AA molecules may strongly interact with the silver in colloids of this metal, undergoing a remarkable fluorescence quenching. The use of an excitation wavelength toward the blue region, i.e., the absorption region of 9AA, allows the selective study of the 9AA not directly linked to the metal by a resonant mechanism, even if the concentration of these 9AA molecules is much lower than that of the chemisorbed 9AA ones, whose photoactivity is highly reduced by the interaction with the metal. Owing to this, we have studied the 9AA/GB complex at 457.9 nm.

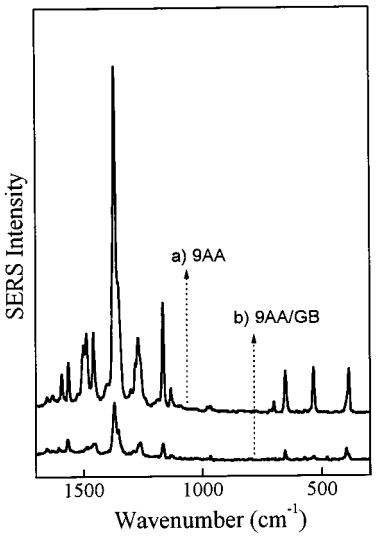

FIGURE 7: (a) SERS spectrum of 9AA (10^{-6} M) and (b) SERS spectrum of the 9AA/GB complex (10^{-6} M 9AA/10^{-5} M GB) by exciting at 457.9 nm.

Figure 6 shows the SERS of the drug (Figure 7a) and the 9AA/GB complex (Figure 7b). The spectra are shown at the absolute intensity at which they were obtained by recording them at the same experimental conditions. The addition of an internal standard was refused to avoid possible interference with complex formation. The first remarkable result that we observed in the SERS of the complex (Figure 7b) was a significant intensity decrease as compared to that of 9AA (Figure 7a), due to the fact that the 9AA interacting with GB is less accessible to the metal surface and, consequently, is further to the surface than the monolayer directly attached to it. As a consequence, the SERS intensity is lower due to the short-range effect of the SERS enhancement also described for other biomolecules (*33*).

Another effect of the interaction with the enzyme is the change observed in the SERS spectral profile. The most significant changes are seen in the 1700−1400 cm^{-1} region (Figure 8). In particular, the bands appearing at 1592, 1501, and 1488 cm^{-1} undergo a marked intensity decrease. According to our previous work (*16*), these bands can be attributed to the imino form of 9AA directly attached to the metal surface. Other interesting effects observed in the complex are the downshift of the 1459 cm^{-1} band, the upshift of the 1564 cm^{-1} band toward 1568 cm^{-1}, and the enhancement of the bands at 1602 and 1655 cm^{-1}. All these bands can be assigned to the amino 9AA tautomer, and may correspond to in-plane C═C and C═N stretching ring

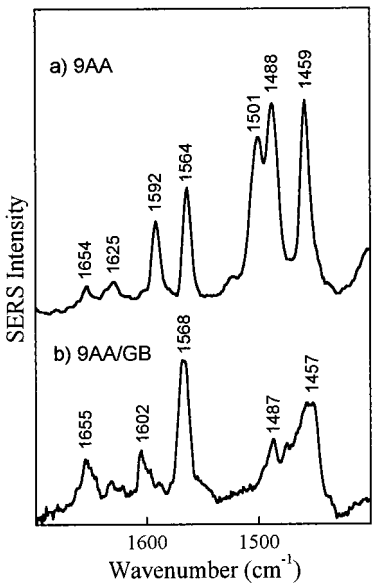

FIGURE 8: SERS spectra of (a) 9AA (10^{-6} M) and (b) 9AA/GB complex (10^{-6} M 9AA/10^{-5} M GB) in the 1400−1300 cm^{-1} region.

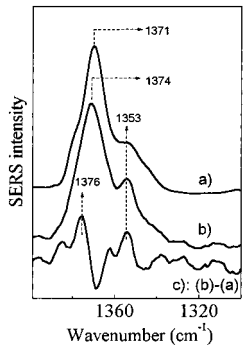

FIGURE 9: SERS spectra of (a) 9AA (10^{-6} M) and (b) 9AA/GB complex (10^{-6} M 9AA/10^{-5} M GB) in the 1700−1400 cm^{-1} region. (c) Difference spectrum between (a) and (b).

vibrations and deformations of the NH_3^+ group. The enhancement of the Raman features corresponding to the amino form together with the strong decrease of the imino Raman features suggests that 9AA interacts with the active center GB under the amino tautomer. As mentioned above, the use of the 457.9 nm line as the excitation wavelength allowed a selective resonant detection of the amino tautomer interacting with GB, although there was more 9AA interacting with the metal surface. The interaction of 9AA with GB under the protonated amino form is consistent with the possible existence in the GB active center of a negatively charge amino acid residue, as has been found for other serine proteases.

In the 1400−1300 cm^{-1} region (Figure 9), where the bands assigned to the collective C═C, C═N, C−N, and C−C vibrations of aromatic rings appear, we observed interesting changes involving the most intense SERS band appearing at 1371 cm^{-1} (Figure 9a) which becomes broader and upshifts to higher wavelengths (Figure 9b), as revealed by a positive band appearing in the difference spectrum of Figure 8c at 1376 cm^{-1}. Moreover, the shoulder appearing at 1353 cm^{-1} in the SERS of 9AA increases in the complex (Figure 9b), appearing as a positive band in the difference spectrum (Figure 9c). The upshift induced by the complexation in the

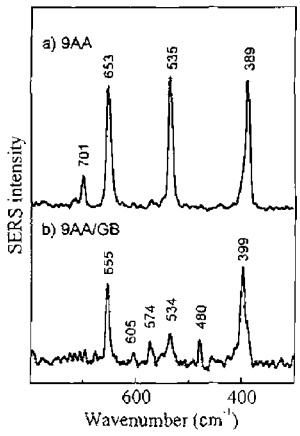

FIGURE 10: SERS spectra of (a) 9AA (10^{-6} M) and (b) 9AA/GB complex (10^{-6} M 9AA/10^{-5} M GB) in the 800−300 cm^{-1} region.

1371 cm^{-1} band may be originated from a electric charge density increase of the $\pi-\pi$ electronic system, associated with a hydrophobic interaction through ring stacking in the complex. Moreover, the intensity increase observed for the band at 1353 cm^{-1} can also be related to such an interaction and to the predominance of the amino tautomer in the complex, since at this wavenumber a band also appears in the SERS spectrum of 9AA recorded at low pH or at high drug concentration, as corresponds to the drug under the protonated amino form (*16*), capable of interacting with a negatively charged amino acid in the active center of GB. The establishment of a ring-stacking interaction in the 9AA/GB complex supports the exciplex emission detected in the emission fluorescent spectra at about 525 nm.

The electrostatic interaction of 9AA through the protonated amino form, as well as the stacking interaction through the aromatic rings, is also reflected in the 800−300 cm^{-1} region (Figure 10). The existence of 9AA in the amino form is demonstrated by the upshift of the band at 389 cm^{-1} to 399 cm^{-1}, which is highly sensitive to the tautomer equilibrium (*16*, *34*). Moreover, the changes observed for other bands of this region (the decrease of the 535 cm^{-1} feature; the appearance of new weak bands at 480, 574, and 605 cm^{-1} ; and the disappearance of that at 701 cm^{-1}) can be attributed to the stacking interaction of 9AA in the 9AA/GB complex, since these bands are mainly attributed to skeletal vibrations of the aromatic systems.

The SERS experiments were also accomplished by using a lower GB concentration: 10^{-6} M. Nevertheless, in this case no difference was observed between the SERS spectrum of the drug in the presence or the absence of enzyme. This result is consistent with the fluorescence spectra obtained for 9AA/GB complexes at 10^{-6} M enzyme concentration (Figure 3), where no significant exciplex emission was detected in the presence of the enzyme, and also suggests the possible enzyme association at 10^{-5} M connected to a structural modification of the drug binding site in GB.

The SERS spectra of the 9AA/GB complex were also studied by using other excitation wavelengths: 514.5 and 1064 nm. The results found with these lines are not shown here because they do not afford important additional information to the conclusions reached with the 457.9 nm excitation. By using the 514.5 nm line, we observed a relative decrease of the 9AA imino bands in the SERS spectrum of

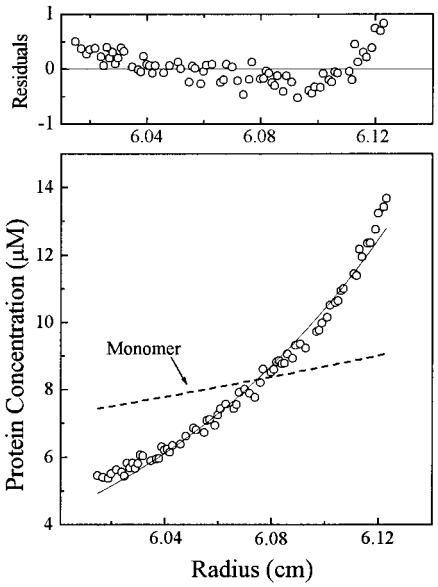

FIGURE 11: Sedimentation equilibrium analysis of GB. Bottom panel: Sedimentation equilibrium gradients of 10 μM GB at 10 krpm as described under Materials and Methods. The symbols represent the experimental data. The solid line shows the fit of the experimental data to a single ideal species. The dashed line corresponds to the theoretical fit to a monomer. Top panel: Residual distribution as a function of the sedimentation distance (this plot corresponds to the difference between the experimental data and the fitted data for each point).

the complex, in the same sense as that observed when using the 457.9 nm line. This again demonstrated the existence of a mixture in the medium: amino 9AA linked to the enzyme and imino 9AA attached to the metal surface. Both tautomers are observed in this SERS spectrum because the amino form is much less resonant at 514.5 nm. Furthermore, at 1064 nm we observed a stronger SERS intensity decrease for the 9AA/GB complex due, in this case, to the absence of a resonance corresponding to the amino 9AA interacting with the enzyme at this excitation line, and the dramatic decrease of imino 9AA adsorbed to the metal, due to the presence of the enzyme. In fact, the weak signal detected in the SERS of the complex obtained at 1064 nm arises from the small amount of 9AA chemisorbed to the surface.

Analytical Ultracentrifugation. As mentioned above, the difference observed in the 9AA fluorescence emission spectra on varying the GB concentration from 10^{-6} to 10^{-5} M can be attributed to a possible polymerization occurring at this concentration range (*14*). To study the association of GB in solution and its dependence on the enzyme concentration, the analytical ultracentrifugation technique was employed.

Sedimentation equilibrium for 10^{-6}–10^{-5} M protein concentrations was carried out. The obtained absorbance gradients were converted to the corresponding weight-average molecular weights with the EQASSOC program ($M_{w,a}$). For all the protein concentrations that were analyzed, the $M_{w,a}$ was quite higher than that of the monomer (70 000), being around 400 000 at 6 krpm and more than 2 times lower (160 000) at 10 krpm. In Figure 11 (bottom), the experimental data are represented together with the ideal sedimentation equilibrium corresponding to a single species. The residual distribution (Figure 11, top) demonstrated the existence of protein aggregation (*35*), but in such a way that the aggregation pattern of GB cannot be fitted to a single species and corresponds to a typical case of multiple polydisperse association (with experimental data forming a *V* up and down of the solid line representing a single species). The existence of association is further demonstrated by comparison of the experimental equilibrium with that of a hypothetical monomer, that is also plotted in Figure 11 (dashed line in the bottom panel). Multiple data sets of apparent weight-average molecular weight vs protein concentration revealed that similar molecular weight distributions were found independently of the GB concentrations. However, the amount of aggregated GB increases on raising the enzyme concentration. All these results point out that this protein is a polydisperse system, in connection to an irreversible association of GB. On the other hand, this behavior is typical of membrane proteins which are expected to aggregate in the absence of membranes, changing their structure and activity as a consequence of this aggregation.

The same experiments were carried out in the presence of 9AA, and the found results indicated that the above aggregation pattern is not significantly affected by the presence of drug, thus corroborating that 9AA does not interact with a GB monomer, which seems to be inactive in terms of interaction with the drug. Experiments of GB activity, using NPGB as substrate, demonstrated that under this monomer form the enzyme does not show any enzymatic activity, thus indicating that the active center of GB is not active in the monomer. This is connected to the fact that the enzyme cannot interact with the drug under the monomeric form, since 9AA binds to the active center of GB. The activity of GB can be observed when increasing its concentration to values where multimer association can occur in solution at a sufficient extent, pointing out that the interaction between monomers induces structural changes which activate the GB catalytic center. In fact, the structure of aggregated GB may resemble that existing in GB when the enzyme is interacting with the cell membrane. The fact that 9AA only shows exciplex emission at a GB concentration of 10^{-5} M reveals, on the one hand, that the drug binds to the enzyme at the catalytic site and, on the other hand, that this drug only interacts with the enzyme under an associated form, at which GB is active. This result is also important under the point of view of the detection of active GB implied in the tumor process, since the exciplex emission of 9AA will only be manifested when GB is active in the cell.

CONCLUSIONS

9AA interacts with GB through the active center of the enzyme. This interaction lead to an exciplex emission, which occurs at a high wavelength (above 500 nm) and only when the enzyme is at a certain concentration (above 10^{-5} M), at which GB is active. This concentration dependence indicates that the drug interacts with the protein only after monomer association, as revealed by analytical ultracentrifugation, due to the activation of the catalytic center upon multimer association. This result allows the application of 9AA in the detection of active GB existing in cells, which is responsible for the tumor metastatic expansion of tumors in tissues, and permits the possible detection of tumor tissues based on a fluorescence probe.

The application of fluorescence and Raman spectroscopies allowed a study of the structural details of the interaction

between 9AA and GB. This interaction takes place at the catalytic center of the enzyme through a mechanism involving two different interactions: electrostatic and ring stacking. The drug interacts with GB under the amino form. Moreover, the active center of GB may be more similar to that of PGA, with a negatively charged amino acid residue and an aromatic residue, whose nature is not yet known, responsible for the hydrophobic ring-stacking interaction leading to the exciplex emission. The interaction of the drug with GB is very selective, as demonstrated by the fluorescence study of the melanoma cells after inactivation of the cytoplasmic enzyme-specific inhibitor. The reversibility of the 9AA/GB interaction, demonstrated by the fluorescence experiments carried out in melanoma cells, corroborates the establishment of a physical interaction between the drug and the enzyme ruling out interaction mechanisms involving a covalent bond or enzyme denaturation.

The structural and molecular details provided by the spectroscopic techniques employed in this work open an interesting research field in the finding of new more powerful inhibitors of GB or other related enzymes, which can be applied both in the detection and in the inhibition of neoplastic processes.

ACKNOWLEDGMENT

We are very grateful to Dr. F. S. Steven for the preparation of samples for fluorescence measurements on human melanoma cells, to Dr. P. Sánchez Mateos for providing melanoma line A375 cells, and to Dr. J. L. Subiza for providing the ascitic fluid of Ehrlich tumor.

REFERENCES

1. Steven, F., Suresh, U., Wong, T. L. H., and Griffin, M. M. (1987) *J. Enzyme Inhibition 1*, 275−287.
2. Poustis-Delpont, C., Descomps, R., Auberger, P., Delque-Bayer, P., Sudaka, P., and Rossi, B. (1992) *Cancer Res. 52*, 3622−3628.
3. Bernstein, L. J., Tonn, J. C., Goldbrunner, R. H., Vince, G. H., Wagner, S., and Goldberg, W. J. (1998) *Anticancer Res. 18*, 2583−2590.
4. Steven, F. S., Anees, M., Talbot, I. C., Blakey, D. C., and Hasleton, P. (1993) *Anticancer Res. 13*, 2003−2010.
5. Zhu, H., Clark, S. M., Benson, S. C., Rye, A. N., and Mathies, R. A. (1994) *Anal. Chem. 66*, 1941−1948.
6. Rehn, C., and Pindur, U. (1996) *Monatsh. Chem. 127*, 645−658.
7. Loechler, E. L., and King, J. (1986) *Biochemistry 25*, 5858−5864.
8. Fornasiero, D., and Kurucsev, T. (1985) *Biophys. Chem. 23*, 31−37.
9. Steven, F. S., Griffin, M. M., Blakey, D. C., Talbot, I. C., Hanski, C., and Bell, J. (1992) *Anticancer Res. 12*, 2159−2164.
10. Steven, F. S., Anees, M., Myers, J., and Hasleton, P. (1993) *Anticancer Res. 13*, 1063−1068.
11. Steven, F. S., Johnson, J., and Eason, P. (1993) *Anticancer Res. 13*, 1059−1062.
12. Steven, F. S., Anees, M., Myers, J., and Hasleton, P. (1993) *Anticancer Res. 13*, 1063−1068.
13. Steven, F. S., Desai, M., Davis, J., Steadman, Y., McClure, J., Eason, P., Palcic, B., and Anderson, G. (1995) *Anticancer Res. 15*, 1521−1525.
14. Poustis-Delpont, C., Thaon, S., Auberger, P., Gerardi-Laffin, C., Sudaka, P., and Rossi, B. (1994) *J. Biol. Chem. 269*, 14666−14671.
15. Thaon, S., Ferrero, C., Auberger, P., Michiels, J. F., Droz, D., Amiel, J. C., Rossi, B., and Poustis-Delpont, C. (1997) *Int. J. Cancer. 72*, 752−757.
16. Murza, A., Sánchez-Cortés, S., and García-Ramos, J. V. (1998) *Biospectroscopy 4*, 327−339.
17. Moskovits, M. (1985) *Rev. Mod. Phys. 57*, 783−826.
18. Murza, A., Robledo, A., Fernandez, R., and Guisan, J. M. (1999) *J Chromatogr. B. 732*, 165−172.
19. Ikkai, T., and Kondo, H. (1996) *J. Biochem. Biophys. Methods 33*, 55−58.
20. Weber, G. (1986) *Biochemistry 25*, 3626−3631.
21. Garbe, C., Krasagakis, K., Zouboulis, C. C., Scroeder, K., Krueger, S., Stadler, R., and Orfanos, C. E. (1990) *J. Invest. Dermatol. 95*, 231S−237S.
22. Zouboulis, C. C., Scroeder, K., Garbe, C., Krasagakis, K., Krueger, S., and Orfanos, C. E. (1990) *J. Invest. Dermatol. 95*, 223S−230S.
23. Steven, F. S., Griffin, M. M., and Al-Ahmad, R. K. (1986) *J Chromatogr. (Biomed. Appl.) 376*, 211−219.
24. Lee, P. C., and Meisel, D. (1982) *J. Phys. Chem. 86*, 3391−3395.
25. Minton, A. P. (1994) in *Modern Analytical Ultracentrifugation* (Schuster, T. M., and Laue, T. M., Eds.) pp 81−93, Birkhäuser, Boston, MA.
26. Gangola, G., Joshi, N. B., and Pant, D. D. (1981) *Chem. Phys. Lett. 80*, 418−421.
27. Grzesiek, S., Otto, H., and Dencher, N. A. (1989) *Biophys. J. 55*, 1101−1109.
28. Fruton, J. S. (1980) *Mol. Cell. Biochem. 32*, 105−114.
29. Angelides, K. J. (1981) *Biochim. Biophys. Acta 669*, 149−156.
30. Lu, W., Apostol, I., Qasim, M. A., Warne, N., Wynn, R., Zhang, W. L., Anderson, S., Chiang, Y. W., Ogin, E., Rothenberg, I., Ryan, K., and Laskowski, M., Jr. (1997) *J. Mol. Biol. 266*, 441−461.
31. Kossiakoff, A. A., and Spencer, S. A. (1981) *Biochemistry 20*, 6462−6474.
32. Karyekar, S. K., and Hedge, M. V. (1991) *Enzyme Microb. Technol. 13*, 139−141.
33. Koglin E., and Séquaris, J. M. (1986) Surface Enhanced Raman Scattering of Biomolecules. in *Topics in Current Chemistry*, pp 1−57, Springer-Verlag, Berlin and Heidelberg.
34. Levi, G., Pantigny, J., Marsault, J. P., and Aubard, P. (1993) *J. Raman Spectrosc., 24*, 745−752.
35. McRorie, D. K., and Voelker, P. J. (1993) *Self-Associating Systems in the Analytical Ultracentrifuge*, Beckman Instruments Inc., Fullerton, CA.

BI000583P